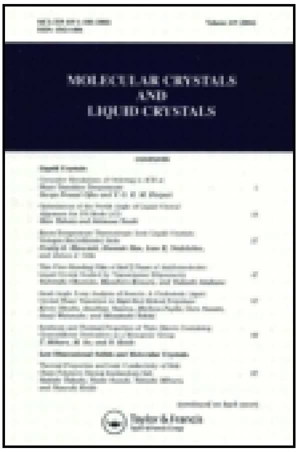

Molecular Crystals and Liquid Crystals
Publication details, including instructions for authors and subscription information:
http://www.tandfonline.com/loi/gmcl20

Field-Directed Diffusion of Charged Lipids in Supported Membranes for Spatially Addressed Microarrays

Yong-Sang Ryu [a], Sang-Wook Lee [a], Byoungho Lee [a] & Sin-Doo Lee [a]
[a] School of Electrical Engineering #032, Seoul National University, Kwanak P.O. Box 34, Seoul, 151-600, Korea

Version of record first published: 11 May 2012.

To cite this article: Yong-Sang Ryu, Sang-Wook Lee, Byoungho Lee & Sin-Doo Lee (2012): Field-Directed Diffusion of Charged Lipids in Supported Membranes for Spatially Addressed Microarrays, Molecular Crystals and Liquid Crystals, 559:1, 1-8

To link to this article: http://dx.doi.org/10.1080/15421406.2012.663522

Mol. Cryst. Liq. Cryst., Vol. 559: pp. 1–8, 2012
Copyright © Taylor & Francis Group, LLC
ISSN: 1542-1406 print/1563-5287 online
DOI: 10.1080/15421406.2012.663522

Field-Directed Diffusion of Charged Lipids in Supported Membranes for Spatially Addressed Microarrays

YONG-SANG RYU, SANG-WOOK LEE, BYOUNGHO LEE,
AND SIN-DOO LEE*

School of Electrical Engineering #032, Seoul National University, Kwanak
P.O. Box 34, Seoul 151-600, Korea

We demonstrated the field-directed diffusion of charged phospholipids in supported bilayer membranes into distributed partitions in a diffusion cell. The balance between the field-induced drift and the thermal Brownian motion generates the concentration gradient of the charged lipids from partition to partition under an external electric field applied longitudinal to the partition walls. The concentration gradient across the partitions was found to primarily depend on the pore width and the distance between the pore and the partition wall. Our field-directed diffusion approach provides a powerful tool for constructing various spatially addressed membrane arrays.

Keywords Charged lipids; field-directed diffusion; lipid composition; spatially addressed; supported membrane

1. Introduction

The development of a versatile platform to achieve well-controlled concentration gradients of amphiphilic molecules showing the liquid crystalline order [1,2], surface-adsorbed species of lipids [3,4] and proteins [5], and DNA associated adsorbates [6] in micropatterned arrays has attracted great attention for systematic studies of biological activities [7–10] including cell adhesion, migration, and growth as well as practical applications [11,12] for axon guidance and chemotaxis. Especially, supported lipid bilayers (SLBs) and model membrane systems reconstituted on solid supports in the charged environment play critical roles on the fundamental studies of membrane-associated activities including cellular deformation [3], vesicle budding [4], signal transduction [6], cell apoptosis [7], and membrane protein trafficking [13].

Recently, microarrays with different concentration profiles of charged lipids in the SLBs have been demonstrated using a number of the fabrication methods, such as a stamping mold [14], the photo-exposure [15], a micropipette [16], and a microfluidic channel [17], that are capable of constructing bilayer arrays with specific composition variations in

---

*Address correspondence to Prof. Sin-Doo Lee, School of Electrical Engineering, Seoul National University, Kwanak P.O. Box 34, Seoul 151-600, Republic of Korea. Tel: +82-2-880-1823; Fax: +82-2-874-9769. E-mail: sidlee@plaza.snu.ac.kr different corrals. However, many of them tend to deform the lipid components physicochemically in the membrane [14] and they often require quite expensive equipments to manipulate the composition variations [15,16].

In this work, we develop a viable, cost-effective scheme of constructing a spatially addressed membrane microarray with partitions wherein different concentrations of charged lipids in a supported bilayer are available within the framework of the field-directed diffusion dynamics. In a diffusion cell composed of a patterned substrate with a pore and partition walls distributed in parallel, the concentration of the charged lipids in each partition depends on the pore size, the distance from the pore to the partition, and an external electric field. It is found that a mechanical scratching method [11] produces the stable and permanent confinement of charged lipids within each partition and thus the concentration gradient is accordingly obtained from partition to partition.

2. Materials and Methods

2.1 Preparation of a Diffusion Cell with Partition Walls

A glass substrate was first cleaned with a solution of piranha [3:1 (v/v) H_2SO_4:H_2O_2] at 120°C for 10 min, followed by ultra-sonication in deionized (DI) water for 10 min. Standard negative photoresist (SU-8 2005, MICROCHEM) was then spun onto the substrate at the spinning rate of 3000 rpm for 30 sec and partition walls were produced as shown in Figs 1(a) and (b). Figure 1b shows the schematic diagram of a diffusion cell having partitions with different concentrations of charged lipids in the SLBs in the presence of an external electric field. The thickness of the SU-8 film was 5 μm which corresponds to the height of a partition wall. Based on the photolithographic technique [10] using an ultraviolet (UV)

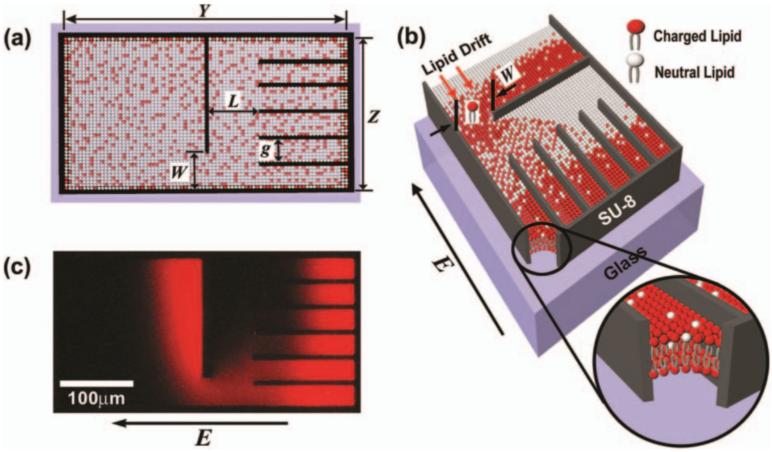

Figure 1. The basic concept of two-dimensional redistribution of charged lipids diffused through a pore (W) in the corner of a diffusion cell into a number of partitions fabricated on a solid substrate: (a) the top view of a diffusion cell with charged lipids (represented in red) distributed at random in the membrane under no external field; (b) a schematic diagram of a diffusion cell showing the redistribution of charged lipids in the presence of an electric field; (c) a fluorescence micrograph showing the redistribution of charged lipids, the Texas Red-DHPEs, in a diffusion cell at the electric field of $E = 45$ V/cm for 20 min.

lamp (MA-6, EVG), the partition walls [represented as thick black stripes in Fig. 1(a)] were fabricated on the glass substrate. A pore of the width W and the partition of the distance L from the pore were shown in Fig. 1(b). The outer side walls of SU-8 were 10 μm thick and the inner partition walls of SU-8 were 4 μm thick. The physical dimensions of the diffusion cell was $Y = 400$ μm and $Z = 200$ μm. The pore width was varies as $W = 10, 20, 40, 60$ μm and the distance from the pore to the inlet of the closest partition was varied as $L = 40$, 60, 80 μm. The gap (g) between two adjacent partitions was fixed to be 30 μm. After the fabrication of the partition walls of SU-8, the diffusion cell was exposed to UV ozone for 10 min to have the hydrophilic surface on which the SLB membrane, separated from the glass support cushioned by a thin (10–20 Å) layer of water [7], was spontaneously formed. For the application of an external electric field to our diffusion cell, two platinum (Pt) wires (each 1.5 cm) were placed outermost sides of the cell along the direction longitudinal to the partition walls. The electric field-directed experiment in our study is similar to the electrophoresis experiment [7]. Across the two Pt wires being used as two electrodes, the direct current electric field of 45 V/cm was applied from a standard power supply. Figure 1(c) shows a typical fluorescence micrograph of the diffusion cell showing the redistribution of negatively charged lipids (the Texas Red-DHPEs) at the electric field $E = 45$ V/cm which was applied for 20 min.

2.2 Forming and Imaging the SLBs

The phospholipids, used as a base for the formation of the SLBs, were 1,2-dioleoyl-sn-glycero-3-phoph-ocholine (DOPC, Avanti Polar Lipids, Birmingham, AL). For imaging the SLBs, negatively charged lipids labeled with red fluorescent dyes, 1,2-dihexadecanoyl-sn-glycero-3-phosp-hoethanola-mine (Texas Red-DHPE, Molecular Probes, Eugene, OR) were mixed with DOPC at 1 mol% (DOPC: Texas Red-DHPE = 99:1). All lipids were dissolved in chloroform. The rapid solvent exchange method [18] was employed to evaporate chloroform and to hydrate with Tris buffer (100 mM NaCl and 10 mM Tris at pH 8.0) simultaneously. Small unilamellar vesicles (SUVs) were produced by extruding 20 times through a 50 nm filter. When the patterned substrate was incubated in the SUV solution, the formation of the SLBs was developed via vesicle adsorption, rupture, and fusion [19]. The residual SUVs remained in the Tris buffer solution were removed with the DI water after the SLBs was fully formed after the substrate was exposed to the SUV solution for 5min. The Texas red lipids were monitored using an epifluorescence microscopy (Eclipse E600-POL, Nikon). The measurements of the fluorescence intensity of fluorescent molecules in SLBs were carried out using an image analyzing program of Image J (National Institute of Mental Health, USA). All the measurements were performed at room temperature.

3. Results and Discussion

The direct current electric field moves negatively charged lipids into the partitions through the pore, starting from the upper corner of the first partition. Due to the electric field-directed diffusion, the neutral lipids (DOPC) are expelled by the charged lipids (Texas Red-DHPEs) from their equlibrium position. The diffusion of Texas Red-DHPEs is governed by the field-induced drift motion with a constant velocity (0.13 ± 0.01 μm/s, estimated from the mid-point trajectory method [6]) and the Brownian motion (with the diffusion constant of 1.0 ± 0.1 μm^2/s, determined from our experimental results of the fluorescence recover after bleaching, which is on the same order of magnitude as in typical lipids [20]). Moreover, since the redistribution of charged lipids depends on the physical dimensions of W and L

in the presence of the electric field, lipid compositions in the SLBs in the partition varies with the lipid distribution profiles in terms of *W* and *L*.

We first vary *W* to be 10, 20, 40, and 60 μm for fixed $L = 60$ μm and measure the distribution profiles of charged lipids at the electric field of 45 V/cm for 20 min. Due to the electric field-directed diffusion, the negatively charged lipids moved into the partitions of P_1 to P_6 and the concentration gradients across the partitions were produced as shown in Figs 2(a), (d). It is clear that the charged lipids were diffused from the pore to the partitions in a continuous manner with different concentration gradients. Figure 2(e) shows the fluorescence intensities for several *W*'s as a function of the transverse distance at the partition edges from P_1 to P_6. Defining the diffusion distance (MDD) as the transverse distance at which the parttion fluorescence intensity becomes zero, the MDD of charged lipids experiencing both the thermal diffusion and the electrical drift are different for different *W*'s. The MDD's represented by $I_0(W)$ were shown in Fig. 2(e). The MDD values for I_0 (10), I_0 (20), I_0 (40) and I_0 (60) [indicated by black arrows in Fig. 2(e)] were about 83, 95, 116 and 134 μm, respectively. As shown in Fig. 2(e), the number of partions with non-vanishing fluorescence intensity increases with increasing *W*. For example, the fluorescence intensity becomes nearly zero in P_3 for $W = 10$ μm while it remains in P_6 for $W = 60$ μm. For membrane arrays with different concentrations of the charged lipids, it is desirable to select the physical dimensions of *W* and *L* that produce both the maximum fluorescence intensity in the first partition (P_1) and the MDD in the mid partition (P_3 or P_4) to give uniform concentration gradients of the charged lipids across the partitions when an equlibrium state is reached after the removal of the the electric field. In our case, the above requirements are satified when $W = 40$ μm for given $L = 60$ μm.

We now vary *L* to be 40, 60 and 80 μm for fixed $W = 60$ μm to examine the dependence of the charged lipid distributions in the partitions on the physical dimension of *L*. Figures 3(a), (b), and (c) are the micropraphs showing the concentration gradients across the partitions for $L = 40$, 60 and 80 μm, respectively. The electric field of 45 V/cm was applied for 20 min. In contrast to Fig. 2 where *W* is varied, the maximum fluorescence intensity is quite indepenent of *L* for given $W = 60$ μm. The results for the concentration profiles of the charged lipids in the partions were similar. The values of the MDD for I_0 (40), I_0 (60), and I_0 (80) were about 105, 134 and 185 μm, respectively [indicated by black arrows in Fig. 3(d)]. As shown in Fig. 3(d), the fluorescence intensity for $L = 40$ μm becomes to zero in P_4 while that for $L = 60$ μm vanishes in P_5. It is interesting to compare the diffusion in the region without partition walls (free diffusion) and that in the partition (restricted diffusion). The lateral diffusion boundary, above which free diffusion is dominant and below which restricted diffusion occurs, is represented by a blue dotted line in Fig. 3(a). Figure 3(e) shows the fluorescence intensities measured in the two regions for $W = 60$ μm and $L = 80$. Away from the outer side wall of the diffusion cell, the fluorescence intensity for free diffusion decays monotonically as a function of the transverse distance while that for restricted diffusion decreases rapidly from P_1 to P_3 and essentially vanishes from P_4 to P_6. This results from the hinderance of the lateral diffusion of the charged lipids in the presence of the partition walls.

We finally demonstrate a spatially adressed membrane arrays with different concentrations of charged lipids in the corrals. The physical dimensions of $W = 60$ μm and $L = 40$ μm were taken on the basis of the above resluts. Figure 4(a) shows the concentration gradients of charged lipids from one partition to other, obtained at the electric field of 45 V/cm for 25 min. The schematic cross-sectional illustration of the distribution of the charged lipids in the last partition P_6 under an electric field is shown in the right side of Fig. 4(a). The concentration gradients measured at the lateral diffusion boundary in the

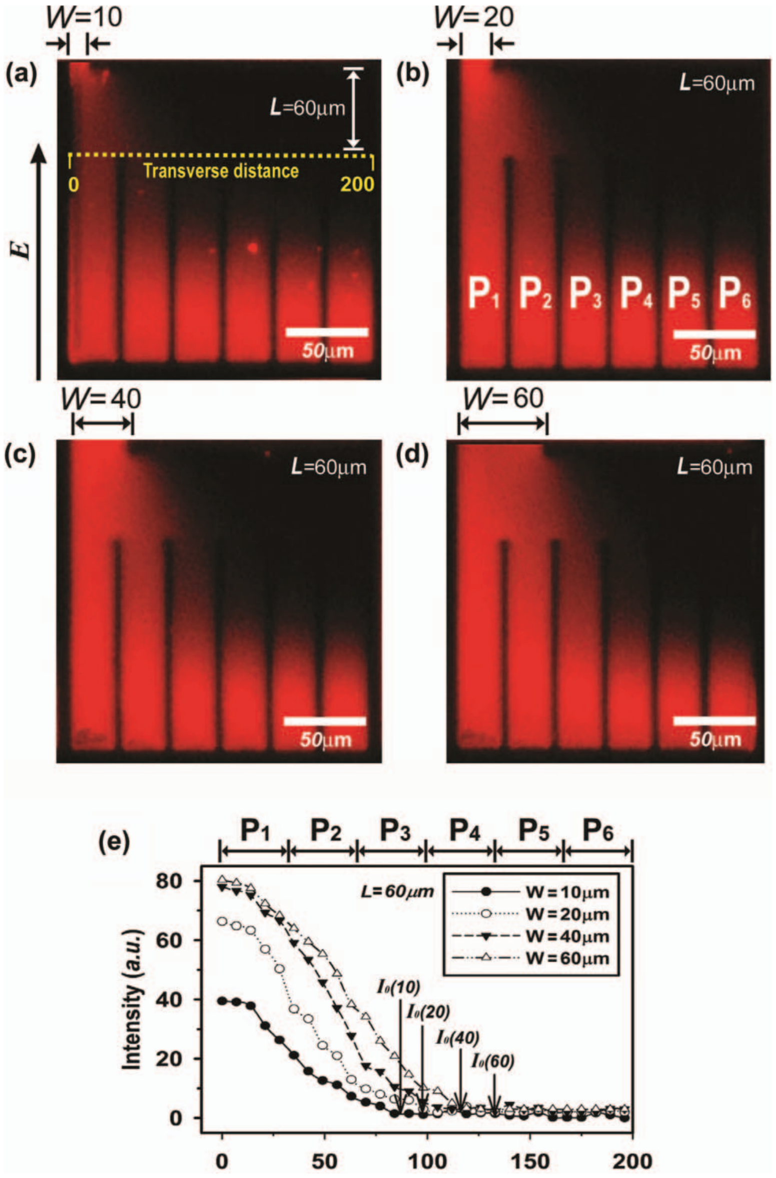

Figure 2. Fluorescence micrographs showing the distribution of charged lipids across the partitions in the membrane for (a) $W = 10$ μm, (b) $W = 20$ μm, (c) $W = 40$ μm, and (d) $W = 60$ μm at $E = 45$ V/cm for 20 min for given $L = 60$ μm. The fluorescence intensity of Texas Red-DHPEs was shown in (e). The maximum diffusion distance (MDD) was represented by I_0 (W).

first (P_1) and the last (P_6) partitions as a function the longitudinal distance (denoted as the yellow dotted line from the bottom to the top) are shown in Fig. 4(b). Note that P_6 shows two regimes, in one of which the gradual change in the concentration of the charged lipids was observed and in the other, essentially no charged lipids were present at the lateral diffusion boundary. After the removal of the electric field, the lipid concentration in the partition will become to be uniform at equilibrium in time. In P_1, no abrupt change in the

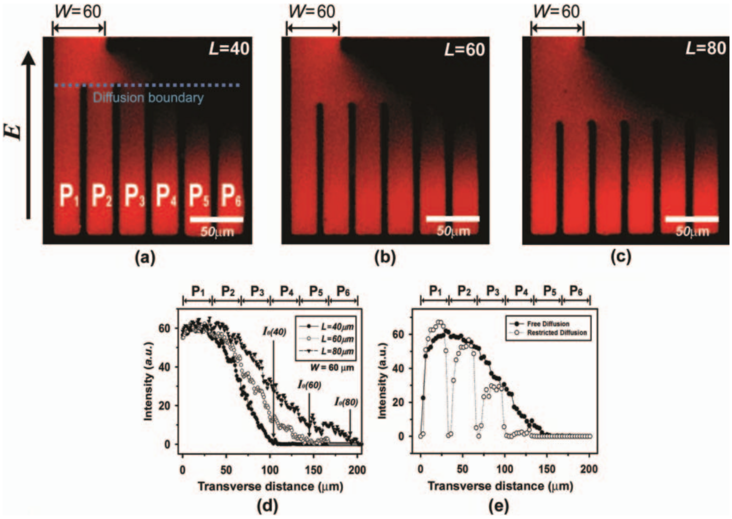

Figure 3. Fluorescence micrographs showing the distribution of charged lipids across the partitions in the membrane for (a) $L = 40$ μm, (b) $L = 60$ μm, and (c) $L = 80$ μm at $E = 45$ V/cm for 20 min for given $W = 60$ μm. The fluorescence intensity of Texas Red-DHPEs was shown in (d). The fluorescence intensities measured in two regions (free diffusion and restricted diffusion in the partition) above and below the lateral diffusion boundary for $W = 60$ μm and $L = 80$ were shown in (e).

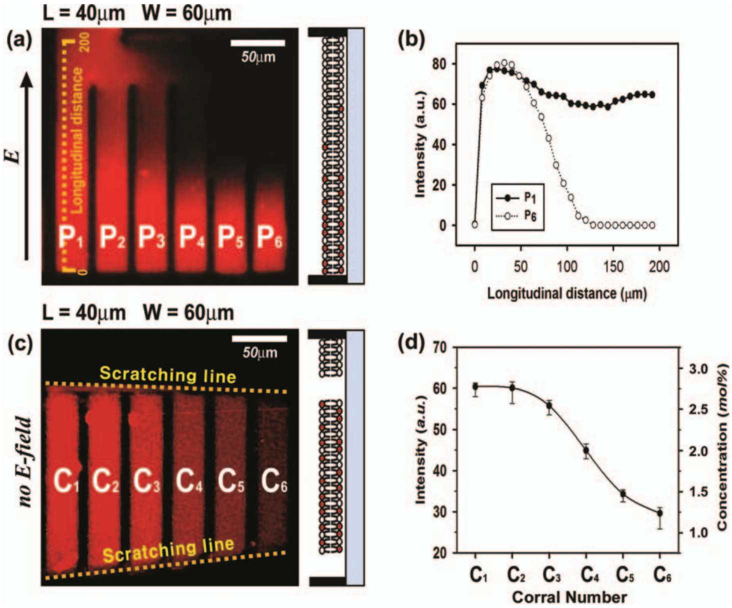

Figure 4. (a) The micrograph showing the concentration gradients of charged lipids from one partition to other for $L = 40$ μm and $W = 60$ μm at the electric field of 45 V/cm for 25 min, (b) the concentration gradients measured at the lateral diffusion boundary in the first (P_1) and the last (P_6) partitions as a function the longitudinal distance, (c) the micrograph showing the confinement of the charged lipids in the corrals with different concentrations by mechanical scratching after the removal of the electric field for 1 h, and (d) the fluorescence intensities and the calculated concentrations of the charged lipids in the corrals from C_1 to C_6.

concentration of the charged lipids was observed along the longitudinal distance. Applying a mechanical scratching method [21] to Fig. 4(a) at 1 hr after the removal of the electric field, a spatially addressed membrane array was obtained as shown in Fig. 4(c) where the charged lipids were permanently confined within the corrals (C_1 to C_6) in the partitions. The scratched lines serve as diffusion barriers for the charged lipids across the corrals. The schematic cross-sectional illustration of the distribution of the charged lipids in the corrals is in the right of Fig. 4(c). Figure 4(d) shows both the fluorescence intensities and the concentrations of the charged lipids, Texas Red-DHPE, in the corrals from C_1 to C_6. Based on the geometrical parameters of the corral such as the size and the height (the gap of the partition) together with the initial concentration of the charged lipids in the SLB, the concentration in each corral was calculated from the fluorescence intensity per volume of the membrane. As an example, for C_6, the estimated concentration of Texas Red-DHPE was 1.25 mol%. As shown in Fig. 4(d), the concentration of the charged lipids can be varied gradually from one corral to the other, being capable of producing a membrane array with different concentrations of the charged lipids. This architecture would be useful for constructing biosensors and developing bioassays for cell culture and growth [10].

4. Concluding Remarks

We developed a viable, cost-effective scheme of constructing a spatially addressed membrane microarray with different concentrations of charged lipids in a supported bilayer from the field-directed diffusion dynamics. In contrast to a direct contact method such as the stamping process [14], our methodology presented here opens a new door to the manipulation of the lipid compositions in the SLB systems and the construction of spatially addressed membrane microarrays with different concentrations of the charged lipids since the field-directed diffusion approach handles the charged lipids in the fluid state in a non-destructive way. Moreover, the partitioning concept presented here can be implemented into microfluidic devices for sorting and positioning colloidal particles [22] and protein molecules [23] using soft lithographic techniques [24,25].

Acknowledgment

This work was supported by the National Research Foundation and the Ministry of Education, Science and Technology of Korea through the Creative Research Initiatives Program (Active Plasmonics Application Systems).

References

[1] Alexandridis, P., Olsson, U., & Lindman, B. (1988). *Langmuir*, *14*, 2627.

[2] Rancon, Y., & Charvolin, J. (1988). *J. Phys. Chem.*, *92*, 2646.

[3] Grakoui, A., Bromley, S. K., Sumen, C., Davis, M. M., Shaw, A. S., Allen, P. M., & Dustin, M. L. (1999). *Science*, *285*, 221.

[4] Sprong, H., van der Sluijs, P., & van Meer, G. (2001). *Nat. Rev. Mol. Cell. Biol.*, *2*, 504.

[5] Fosser, K. A., & Nuzzo, R. G. (2003). *Anal. Chem.*, *75*, 5775.

[6] Groves, J. T., Wülfing, C., & Boxer, S. G. (1996). *Biophys. J.*, *71*, 2716.

[7] Waring, P., Lambert, D., Sjaarda, A., Hurne1, A., & Beaver, J. (1999). *Cell Death and Differentiation*, *6*, 624.

[8] Barrett, E. W., Phelps, M. V. B., Silva, R. J., Gaumond, R. P., & Allcock, H. R. (2005). *Biomacromolecules*, *6*, 1689.

[9] Nakanishi, J., Kikuchi, Y., Inoue, S., Yamaguchi, K., Takarada, T., & Maeda, M. (2007). *J. Am. Chem. Soc.*, *129*, 6694.

[10] Groves, J. T., Mahal, L. K., & Bertozzi, C. R. (2001). *Langmuir*, *17*, 5129.

[11] Knapp, D. M., Helou, E. F., & Tranquillo, R. T. (1999). *Exp. Cell Res.*, *247*, 543.

[12] Baier, H., & Bonhoeffer, F. (1992). *Science*, *255*, 472.

[13] De Vrije, G. J., Batenburg, A. M., Killian, J. A., & De Kruijff, B. (1990). *Mol. Microbiol.*, *4*, 143.

[14] Kung, L. A., Groves, J. T., Ulman, N., & Boxer, S. G. (2000). *Adv. Mater.*, *12*, 731.

[15] Hovis, J. S., & Boxer, S. G. (2000). *Langmuir*, *16*, 894.

[16] Cremer, P. S., & Yang, T. J. (1999). *J. Am. Chem. Soc.*, *121*, 8130.

[17] Groves, J. T., & Boxer, S. G. (2002). *Acc. Chem. Res.*, *35*, 149.

[18] Lee, S.-W., Jeong, C., & Lee, S.-D. (2009). *J. Phys. Chem. B*, *113*, 3610.

[19] Yoon, T.-Y., Jeong, C., Kim, J. H., Choi, M. C., Kim, M. W., & Lee, S.-D. (2004). *Appl. Surf. Sci.*, *238*, 299.

[20] Yee, C. K., Amweg, M. L., & Parikh, A. N. (2004). *Adv. Mater.*, *16*, 1184.

[21] Cremer, P. S., Groves, J. T., Kung, L.A., & Boxer, S.G. (1999). *Langmuir*, *15*, 3893.

[22] Na, Y.-J., Yoon, T.-Y, Park, S., Lee, B., & Lee, S.-D. (2010). *Chem. Phys. Chem.*, *11*, 101.

[23] Fosser, K. A., & Nuzzo, R. G. (2003). *Anal. Chem.*, *75*, 5775.

[24] Xia, Y., & Whitesides, G. M. (1988). *Angew. Chem. Int. Ed.*, *37*, 550.

[25] Haeberle, S., & Zengerle, R. (2007). *Lab on Chip*, *7*, 1094.